Bioelectrochemistry 74 (2008) 118–123

Contents lists available at ScienceDirect

Bioelectrochemistry

journal homepage: www.elsevier.com/locate/bioelechem

Amyloid-β detection with saccharide immobilized gold nanoparticle on carbon electrode

Miyuki Chikae [a], Tomohiro Fukuda [a], Kagan Kerman [a], Koutarou Idegami [b], Yoshiko Miura [a], Eiichi Tamiya [c,*]

[a] School of Materials Science, Japan Advanced Institute of Science and Technology, 1-1 Asahidai, Nomi City, Ishikawa 923-1292, Japan
[b] Ishikawa Sunrise Industries CreationOrganization, 2-20 Kuratsuki, Kanazawa City, Ishikawa 920-8203, Japan
[c] Department of Applied Physics, Graduate School of Engineering Osaka University, 2-1 Yamadaoka, Suita, Osaka 565-0871, Japan

ARTICLE INFO

Article history:
Received 29 January 2008
Received in revised form 15 May 2008
Accepted 2 June 2008
Available online 12 June 2008

Keyword:
Sialic acid
Biosensor
Alzheimer's amyloid-β peptide
Gold nanoparticle
Self-assembled monolayer
Voltammetry

ABSTRACT

The electrochemical sensing of saccharide–protein interactions using a couple of sialic acid derivatives and Alzheimer's amyloid-beta (Aβ) is described. The densely-packed saccharide area for recognition of protein was fabricated onto a carbon electrode by three steps, which were electrochemical deposition of Au nanoparticles on a screen printed strip, self-assembled monolayer (SAM) formation of the acetylenyl group on Au nanoparticles, and the cycloaddition reaction of an azide-terminated sialic acid to the acetylenyl group. The attachment of Aβ peptides to the sialic acid layer was confirmed by electrochemistry and atomic force microscopy imaging. The intrinsic oxidation signal of the captured Aβ(1-40) and (1-42) peptides, containing a single tyrosine (Tyr) residues, was monitored at a peak potential of 0.6 V (vs Ag/AgCl within this sensor) in connection with differential pulse voltammetry. The peak current intensities were concentration dependent. The proposed process provides new routes for analysis of saccharide–protein interactions and electrochemical biosensor development.

1. Introduction

Saccharides, which are widely expressed on the cell surfaces, play a crucial role in various biological recognition events such as infection of pathogens and occurrence of disease [1]. Therefore, saccharides and their derivatives are useful as bio-recognizable materials for biosensor [2]. Since the saccharide–protein interactions are usually weak, the ingenious device is needed to apply the interaction for the sensor apparatus. The saccharide–protein interaction can be amplified by glyco-cluster effect of multivalency [3], and the saccharide assembly by liposome [4], LB membrane [5] and self-assembled monolayer (SAM) [6] are utilized for the biosensor.

In particular, the cabohydrate-immobilized substrate is suitable for the bioanalysis, because it exhibits the large glyco-cluster effect and can be detected by the sensitive analytical methods [7–10]. The sensitivity of the cabohydrate-immobilized substrate can be improved by substrates. Especially, Au nanoparticles have been extensively used as matrices and cytochemical labels for the immobilization and study of biomolecules due to the high sensitivity based on the larger surface area and the applicability to the various detection method by the metallic properties.

The immobilization of densely packed saccharides is essential for the fabrication of biosensig device. There are several strategies for immobilization like LB membrane [5] and SAMs [6]. The LB membrane formation is possible only on the clean flat substrate. On the other hand, the SAM can be formed on the various substances including nanoparticles. In addition, the chemical transformation of the functional SAM also can be utilized for the saccharide immobilization. We have reported the saccharide-immobilization by the SAMs formation of disulfide compounds and by the chemical transformation on the substrate via a click reaction [11,12]. Considering the facile preparation of saccharide, the SAM formation and the consequent chemical transformation are useful and universal.

The detection of saccharide–protein interactions has been reported by surface plasmon resonance (SPR), [7] quartz crystal microbalance (QCM) [8], and evanescent-field fluorescence [9]. These detection techniques have enough sensitivity, but the sensing devices are too expensive. The electrochemical detection of them has an advantage for the applicability and the development of low-cost devices. However, the electrochemical detection is difficult with the densely packed saccharides structure due to the insulating properties. For this aim, we fabricated a new functional carbon electrode including the densely packed saccharides area and electroactive bare carbon area, and demonstrate for electrochemical sensing of saccharide–protein interactions using a couple of sialic acid derivatives and Alzheimer's amyloid-beta (Aβ) peptides as a model case.

* Corresponding author. Tel.: +81 6 6879 4087; fax: +81 6 6879 7840.
E-mail address: tamiya@ap.eng.osaka-u.ac.jp (E. Tamiya).

1567-5394/$ – see front matter © 2008 Elsevier B.V. All rights reserved.
doi:10.1016/j.bioelechem.2008.06.005

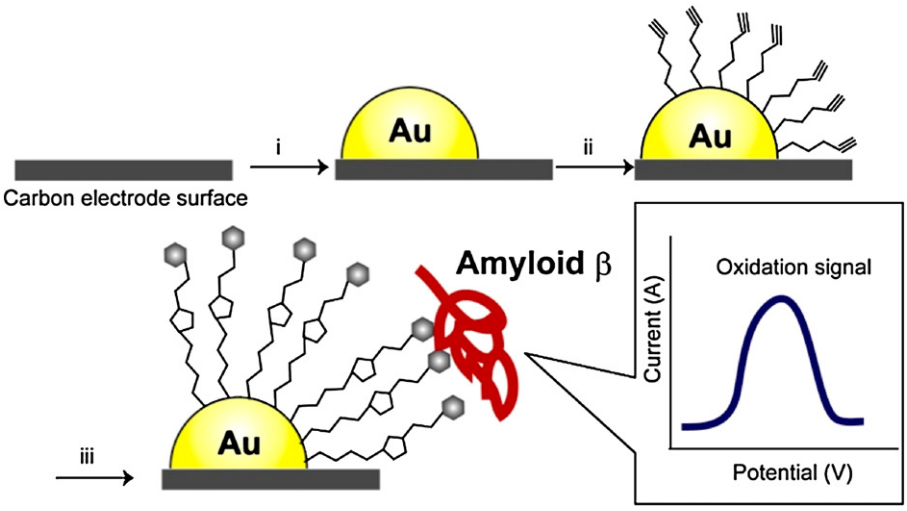

Scheme 1. Schematic illustration of the nanobioelectronic detection system for Alzheimer's Aβ peptides. The sugar immobilized substrate was prepared through i-iii steps (i) deposition of gold nanoparticle on carbon electrode, ii) formation of acetylenyl-terminated self-assembled monolayer, and iii) saccharide immobilization for Aβ detection.) The attachment of Aβ peptide to the sugar layer and the electrochemical detection were realized on a single electrode. The peak oxidation current response of Tyr residue of Aβ was utilized as the analytical signal.

There are a number of saccharides including monosaccharide, oligosaccharide, glycoprotein, glycolipid and proteoglycan, but only the core saccharide structure is necessary for biosensing and biomaterials [13]. For example, the sialic acid (*N*-acetyl-D-neuraminic acid) conjugate with polydiacetylene was reported to detect influenza virus [14]. The globobiose-immobilized substrate was utilized for Shiga toxin detection [15]. Recently, it has been revealed that the cell-surface saccharides are related to the Alzheimer disease [16]. Alzheimer disease is occurred by aggregation of amyloid-beta (Aβ) peptides, and the aggregation has been reported to relate to the interaction with ganglioside (GM1). The sialic acid is an essential element of ganglioside [17], and so it is expected that the Aβ can be detected using sialic acid. It is expected that sialic acid SAM enables the binding with Aβ and provides a chemically stable and cost-effective recognition interface for Aβ.

Voltammetric detection of tyrosine (Tyr) has been exploited in several label-free protein sensor schemes [18–20]. Interestingly, Aβ peptides have one Tyr residues in the protein. We have monitored the oxidation of the single Tyr residue in Aβ peptides as the analytical signal in this sensor, and reported a label-free monitoring method for Aβ aggregation using the oxidation signal of Tyr on a glassy carbon electrode [21].

In this study, we propose a new protocol of electrochemical sensing of saccharide–protein interaction as illustrated in Scheme 1. Acetylenyl-terminated SAM was formed on Au nanoparticle-electrodeposited a screen-printed carbon strips (SPCS), azide-linked sialic acids were reacted with an acetylenyl-terminated SAM using the 1, 3-dipolar cycloaddition (Scheme 2). Aβ was captured by the specific interaction between the peptide and the densely-packed sialic acid. The oxidation signal of Tyr from the captured Aβ was investigated using differential pulse voltammetry (DPV). The interactions between the multiple sialic acid and Aβ peptide were conformed by atomic force microscopy.

2. Experimental section

2.1. Reagents and chemicals

The following reagents were used as received: Sodium *L*-ascorbate, $HAuCl_4 \cdot 3H_2O$, Copper (II) sulfate, triethylene glycol, potassium carbonate, 3-bromopropyne, sodium hydrate, trichloroisocyanuric acid, iodomethane, were products of Kanto Kagaku Co. (Japan). 11-bromo-1-undecene, 2,2′-azobis (isobutyronitrile) (AIBN), $K_3[Fe(CN)_6]$, HCl, Na_2HPO_4, NaH_2PO_4, KOH, polyvinylalchol, NH_4OH and dimetylsulfoxide (DMSO) were purchased from Wako Pure Chemical (Japan). Thioacetic acid were purchased from Tokyo Kasei (Japan). Amyloid-beta (Aβ) peptides (Aβ-(1-40), and Aβ-(1-42); trifluoroacetate form) were purchased from Peptide Institute Inc. (Japan). All other solvent

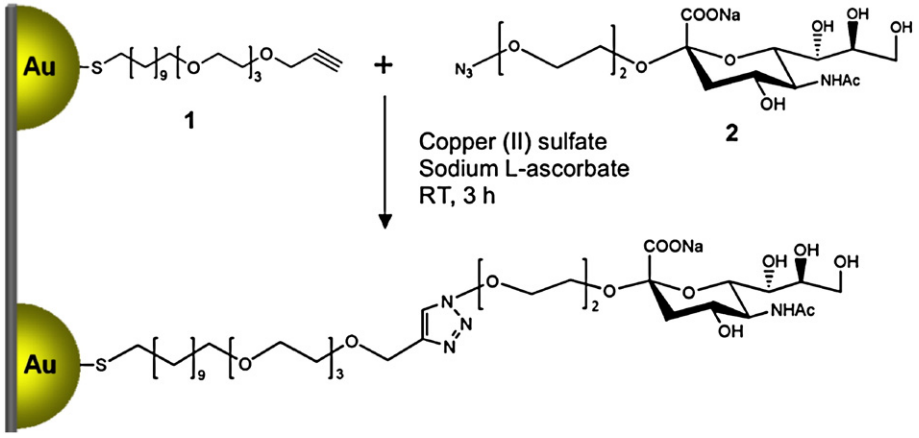

Scheme 2. The addition of azide-linked sialic acid to acetylenyl-terminated SAM using 1,3-dipole cycloaddition reaction on the surface of Au nanoparticles.

and chemicals were of analytical grade. All solutions were prepared and diluted using ultra-pure water (18.3 MΩ cm).

2.2. Instrumental

Electrodeposition and measurements, in connection with chronocoulometry (CC), cyclic voltammetry (CV), and differential pulse voltammery (DPV) were performed using a Autolab PGSTAT 12 electrochemical analysis system (Eco Chemie, The Netherlands) with General Purpose Electrochemical System (GPES) software. The planar screen-printed carbon strip (SPCS) and screen-printed gold strip were provided from BioDevice Technology Ltd. (Japan). These are consisted of a carbon/gold working electrode (geometric working area: 2.64 mm^2), a carbon counter electrode, and Ag/AgCl reference electrode. Electrochemical deposition and measurements were performed in 30 μL of the solution covering all three electrodes in a horizontal position. All measurements were carried out at a controlled room temperature. Atomic force microscopy (AFM) was performed in air with a commercial unit (SPA400, Seiko Instruments Inc., Japan) equipped with a calibrated 20 μm *xy*-scan and 10 μm *z*-scan range PZT-scanner. Silicon nitride tip (SI-DF20, spring constant = 15 N/m, Seiko Instruments Inc.) was used, and images were taken in a dynamic force mode (DFM mode) at an optimal force. Gold substrates, named Auro sheet (1, 1, 1) HS, were purchased from Tanaka Kikinzoku Co. (Japan) for AFM measurements. FTIR spectra were recorded on a JASCO FTIR-4000 Fourier transform infrared spectrometer, and for RAS measurement, a Harrick model Refractor 2 reflection attachment was used. Thickness of the layer was measured with a ellipsometer DVA-FR (Mizojiri Kogaku, Japan). FTIR and ellipsometery was measured using the gold substrate (Moritex, Japan).

2.3. Synthesis of the component molecules

Acetylenyl-terminated disulfide for SAM forming molecule was synthesized from triethylene glycol according to the manner reported by Lee et al. [11]. Briefly, the substitution reaction with 11-bromo-1-undecene, subsequent addition of thioacetic acid, and migration of acetyl group from thiol to the hydroxyl group by the treatment of sodium hydride leaded to disulfide compound with acetyl terminal. The acetyl-terminated compound was converted to acetylenyl terminal production by the deprotection using potassium carbonate, and the alkylation of propargyl bromide. Azide-linked sialic acid was obtained by the conventional saccharide synthesis [22].

2.4. Fabrication of the Aβ sensor

The Au nanoparticles were electrodeposited on the carbon based working electrode included the screen-printed strips according to the same manner described previously [23] with slightly modification. The electrodepositions of gold were performed in the 30 μL of the solution, 1 mM $HAuCl_4$ in 0.1 M HCl, covering all three electrodes while applying a potential of 0.3 V (vs Ag/AgCl within SPCS) during 200 s. The treated SPCS was rinsed using ultra-pure water, and blot-dried.

For fabrication of the acetylenyl-terminated SAMs on the SCPS, 2 μL of 5 mM acetylenyl-terminated disulfide in 50 mM Tris–HCl buffer (pH 8.0) was dropped over the nano-gold deposited working electrode for 12 h under the water-saturated atmosphere. The electrode surface was rinsed with an ethanol and ultra-pure water, and blot-dried.

Azide-linked sialic acid was immobilized by 1,3-dipole cycloaddition (click chemistry) on the acetylenyl-terminated SAMs in Scheme 2. Aliquot of 2 μl of the mixture containing 10 mM azide-linked sialic acid, 50 mM $CuSO_4$ and 125 mM sodium *L*-ascorbate was dropped on the working electrode, in which the acetylenyl-terminated SAMs on the nano-gold was distributed for 3 h under the water saturated atmosphere. After rinsing by ultra-pure water, the electrode surface was cleaned by the treatment of DPV (applied potential: from 0 V to 1 V, step potential: 5 mV) in blank PBS.

Finally, the remained carbon surfaces were blocked by 20 ml of 1% polyvinylalcohol for 10 min due to avoid the non-specific adsorption. These strips were rinsed by ultra-pure water and kept under 4 °C until use.

2.5. Detection of the Aβ

As a stock solution, 200 μM Aβ(1-40) and Aβ(1-42) in 0.02% of NH_4OH were prepared and kept at 4 °C. The test sample was diluted by Aβ assay buffer (20 mM phosphate buffer (pH 7.5) containing 100 mM NaCl) from stock solution just before treatment to avoid the Aβ aggregation. Aliquot of 20 μL test sample was applied to the sensor strip with mild rolling (80–100 rpm). After washing step by PBS, the captured Aβ was detected by the oxidation signal of tyrosine by DPV (applied potential: from 0.2 V to 0.8 V vs Ag/AgCl within SPCS, step potential: 5 mV, amplitude: 75 mV). The raw voltammograms of DPV were treated by using Savitzky-Golay smoothing (level 4) and the "moving average" baseline correction of GPES with a peak width of 0.005 V. The electrochemical measurements were performed for 3 times for each condition ($n = 3$) except otherwise stated.

3. Results and discussion

3.1. Characterization of the partial SAM on the carbon electrode

Previously, we have demonstrated the fabrication of Au nanoparticles on SPCSs using electrodeposition [23]. Size, shape, and number of Au nanoparticles could be controlled by varying the concentration of $[AuCl_4]^-$ and the applied potential and time in electrodeposition treatment. After applying a potential of 0.3 V vs Ag/AgCl for 200 s using 30 μL of 1 mM $HAuCl_4$ in 0.1 M HCl, the change in the color of the carbon-based working electrode area became visible to the naked eye. The electrodeposited Au nanoparticles could also be observed using SEM (Fig. 1).

The reductive deposition of acetylenyl-terminated disulfide (1) on Au nanoparticles was demonstrated using CV from −0.6 to −1.8 V vs Ag/AgCl (scan rate; 0.1 mV/s) in 0.5 M KOH. It was well-described that SAMs on Au showed several characteristic voltammetric waves in response to their reductive deposition [24,25]. In this case, the reduction signal of the Au–S binding to electrodeposited Au were observed at −1.4 V vs Ag/Ag/Cl (Fig. 2A). Additionally, the peak current intensities increased according to the electrodeposition time (0, 30, and 200 s), which could be attributed to the increase in the electrodeposited Au volume. Therefore, the SAM formation with alkyl disulfide on the

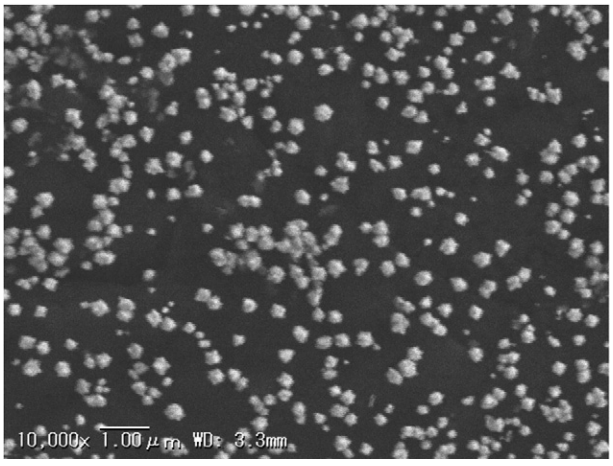

Fig. 1. SEM image of the electrodeposited Au nanoparticles on the carbon-based working electrode of SPCS. Electrodeposition was performed at the potential of 0.3 V vs Ag/AgCl within the SPCS during 200 s using 30 μL of 1 mM $HAuCl_4$ in 0.1 M HCl.

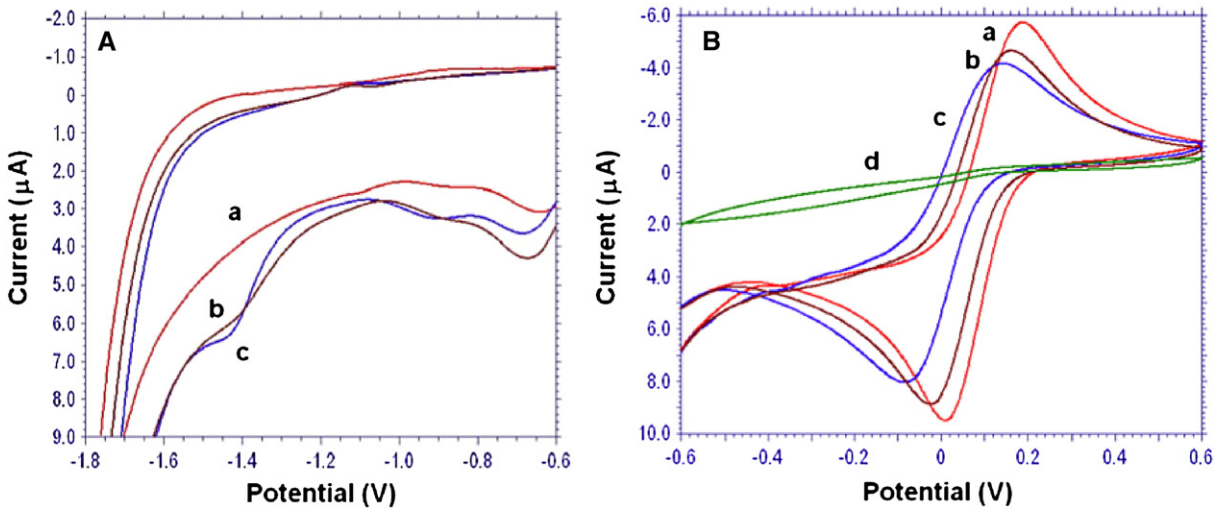

Fig. 2. Cyclic voltammograms of partial SAM formed on SPCSs in 0.5 M KOH from 0 to −1.8 V vs Ag/AgCl within the SPCS at 0.1 V/s (A), and in 2 mM $K_3[Fe(CN)_6]$ in PBS (pH 7.4) from −0.6 to 0.6 V at 0.1 V/s (B). Electrodeposition time was 0 s (a), 30 s (b), and 200 s (c); whereas (d) shows the response obtained using a screen-printed Au strip (SPGS) after 200 s electrodeposition and consequent full surface coverage with SAM formation.

electrodeposited Au nanoparticle could be estimated, and the dispersed dotted SAMs on the carbon electrode with acetylene group were subject to the saccharide modification.

It is well-defined that a SAM can form a lipophilic barrier for electron transfer between the electrode surface and the hydrophilic electroactive probes in solution [26–28]. Fig. 2B-a to c show the cyclic voltammograms of 2 mM $K_3[Fe(CN)_6]$ in PBS at the partial SAM on carbon strips. The peak current intensities of the redox decreased as the electrodeposition time (0, 30, and 200 s) of Au nanoparticles. It indicates that the electron transfer at the treated SPCS became blocked according to the amount of the electrodeposited Au nanoparticles and the SAM formation. In the case of a screen-printed Au strip (SPGS), the redox activity was inhibited by the monolayer formed using the same treatment (Fig. 2B-d). From these observations, we could control and maintain the electron transfer activity of SAM formed electrode using the preparation protocol described above in the Experimental section.

The subsequent sialic acid deposition via a click chemistry was confirmed in detail by XPS, FTIR-RAS, contact angle and ellipsometry measurements, though the CV measurements of the sialic acid deposition didn't show the clear difference from that before the click reaction (Supplementary data). The C1s spectra of the layer was measured by XPS. The main peak around 286 eV was observed, where the shoulder peak around 287 eV indicated C–O of sialic acid and ether unit of SAM. The FTIR showed typical bands of saccharide moieties (3100–3500 cm^{-1} (νOH)). The ellipsometry showed the thickness of acetylenyl-terminated SAM, 20 Å and the thickness of sialic acid layer was 4.5 Å. The contact angle was almost the same on the partial SAM and the sialic acid substrate about 52°. We have reported the saccharide immobilization by click chemistry. The chemical transformation of monosaccharide proceeded quantitatively on the SAM of gold substrate as well.

This SAMs on SPCS realized the immobilization of the biomaterials (Au area) and the electrochemical detection (carbon area) in one electrode. The covalent bond formation with click chemistry can be applied to the many kinds of biomolecules such as enzyme, antibody, and DNA. Therefore, the combination of the specific reaction of the biomaterial on the SAMs and following the electrochemical detection could be able to extend to many biosensing devices.

3.2. Evaluation of the Aβ sensor

The interaction between Aβ and the sialic acids layer were investigated using AFM in the same manner as described for the Au nanoparticles [23]. The surface of Au substrate was smooth (Fig. 3A). After modification with sialic acid, Au substrate showed a slight roughness due to the rearrangement of gold atoms via a chemical reaction (Fig. 3B) [29]. The attachment of Aβs was observed with applying 20 mM of the samples. Fig. 3C and D showed rougher surface than the sialic acid-modified surface, meaning the attachment of Aβ(1-40) and Aβ(1-42) on the sialic acid layer after 180 min incubation. The morphology of Aβ(1-40) was small round aggregates with 10–100 nm diameter (Fig. 3C). The morphology of Aβ(1-42) was a slight different from that of Aβ(1-40), which was a mixture of small round object with 10–100 nm and amyloid fibrils with 70–150 nm in diameter and over 500 nm in length. The AFM observation indicated the affinity of sialic acid to Aβ peptides, and the aggregation properties of Aβ peptides. The round object of Aβ is considered to be the self-assembling structure of ADDL (amyloid-derived diffusible ligands) [30], suggesting the ADDL formation on ganglioside.

The oxidation peak current intensity of Aβ peptide on the sensor was observed at 0.6 V (vs.Ag/AgCl within this sensor) (Fig. 4A) in agreement with our previous reports [18–21]. There was no difference in the oxidation potential between 5 μM Aβ(1-40) and 5 μM Aβ(1-42). The peak current of Aβ(1-40) was increased according to the applied Aβ concentration from 0.5 μM, reached maximum at 10 μM, and then slightly decreased in the higher concentration. The peak current of Aβ(1-42) showed the similar tendency to Aβ(1-40). The peak current was observed from 0.5 μM, and almost saturated at 10 μM. The intensities of peak current of Aβ(1-42) were a little smaller than those of Aβ(1-40), and the peak current deviation of Aβ(1-42) was larger than that of Aβ(1-40). Those difference between Aβ(1-40) and (1-42) was caused by the aggregation properties of Aβ(1-42) and the stiff structure of Aβ(1-42) aggregates [21]. Both peptides had a detection limit of 1 μM calculated from three times of the standard deviation.

Moreover, Aβ(1-40) applied to the device, which was fabricated by the same process on a screen-printed Au strip (SPGS). However, Tyr oxidation signal could not be observed due to the weak affinity of Aβ to Au electrode (data not shown), indicating the interface modification much affects the sensitivity. Our results indicated the sensitivity for Aβ detection was much improved by the sialic acid modification on SPGS based on the saccharide-Aβ interaction. The interaction of ganglioside such as GM1 with Aβ peptides, and the aggregation properties of Aβ on the acidic group immobilized substrate were reported [17]. The sialic acid has a simple structure comparing to ganglioside, but was essential structure for Aβ binding. The sialic acid modified substrate amplified the affinity to Aβ peptides, as designed.

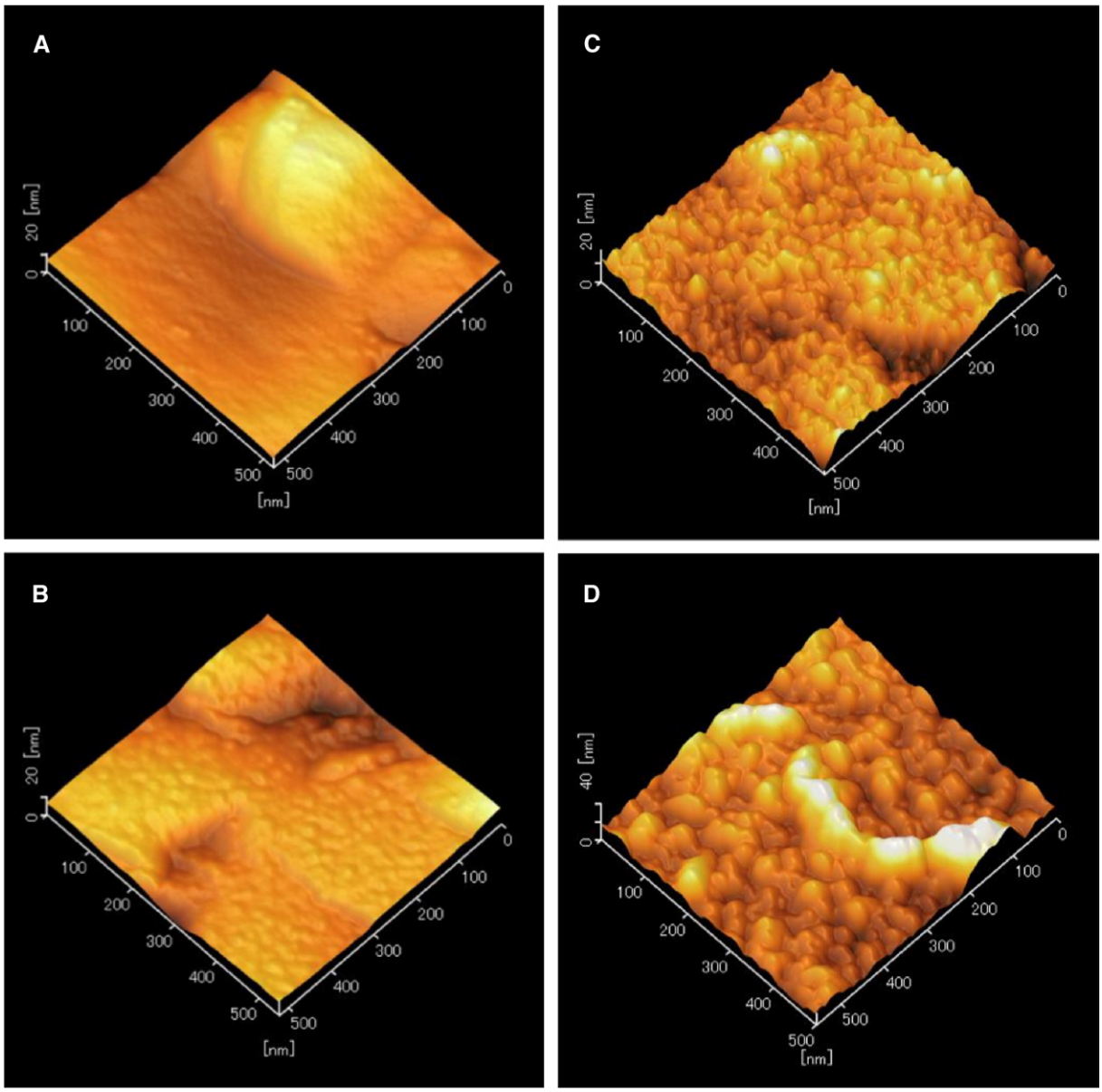

Fig. 3. AFM images of the bare gold substrate (A); after cycroaddition of the sialic acid (B); the attachment of 20 μM Aβ peptides after incubation at RT for 180 min; Aβ(1-40) (C) and Aβ(1-42) (D).

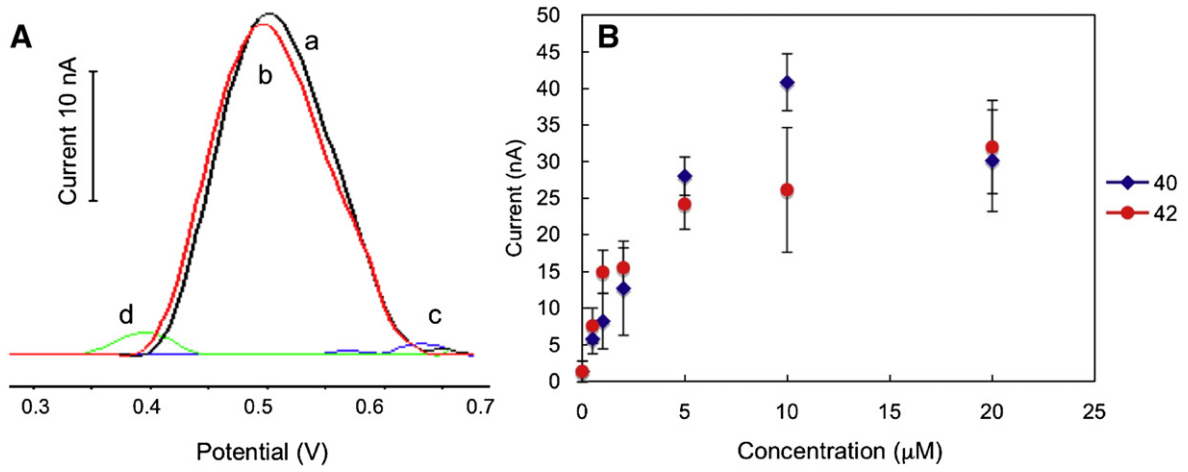

Fig. 4. Electric responses of the Aβ sensor applied the Aβs. Aβ(1-40) (a), Aβ(1-42) (b), insuline (c) from 5 μM solutions, and PBS only (d) (A). The relationship between the Aβ peptides concentrations and the current determined by this Aβ sensor. Each data indicate the average of 3 measurements with the error bars indicating the relative standard deviation (B).

On the other hand, other proteins were also measured to investigate the detection specificity. When 0.1% bovine serum albumin in PBS (pH 7.4) was applied as a negative control, no oxidation signal of Tyr was observed. The addition of insuline also didn't show any Tyr current, even though insulin has four Tyr residue, meaning the interaction of insulin to sialic acid was too little to detect the signal (Fig. 4A). The saccharide-modified surface has been reported to show the specific binding to proteins, and the surface shows the inner surface properties except specific proteins [31]. Even though some proteins, viruses and bacteria show the binding to sialic acid [1], the saccharide-modified substrate showed the enough specificity to Aβ detection in this research. The unique electrochemical properties of Aβ in Tyr current and impedance can help the specific detection, which is still under way.

Current effort in our laboratory aims at the sensing more pathogens, such as Shiga toxins, and influenza virus, and at the evaluation of various synthetic saccharide derivatives. On the other hand, the immobilization of the saccharides as the biorecognition materials on electrodes provides new routes for electrochemical biosensor development. The label-free detection of Aβ peptide was demonstrated here as a model case, and further excellent labeling systems promises the development of highly sensitive sensors.

4. Conclusions

Considering the glycoside cluster effect, the immobilization of the saccharides as the biorecognision materials on carbon electrodes provides new routes for analysis of saccharide–protein interactions and electrochemical biosensor development. Synthetic monosaccharide, sialic acid, for the recognition of Aβ peptides could be introduced densely over the partial SAM on the carbon electrode via the electrodeposited Au nanoparticles. The coexistence both Au nanoparticles for the immobilization of biomolecules and bare carbon for electrochemical detection on the electrode enables the electrochemical sensing with easy fabrication and low-cost. Our proposed process offers further applications of electrochemical sensing of saccharide–protein interactions.

Appendix A. Supplementary data

Supplementary data associated with this article can be found, in the online version, at doi:10.1016/j.bioelechem.2008.06.005.

References

[1] A. Varki, Biological roles of oligosaccharides: all of the theories are correct, Glycobiology 3 (1993) 97–130.
[2] R. Jelinek, S. Kolusheva, Saccharide biosensors, Chem. Rev. 104 (2004) 5987–6015.
[3] Y.C. Lee, R.T. Lee, Saccharide–protein interactions: basis of glycobiology, Acc. Chem. Res. 28 (1995) 321–327.
[4] S. Ahn-Yoon, T.R. DeCory, A.J. Baeumner, R.A. Durst, Gangliosides-liposome immunoassay for the ultrasensitive detection of cholera toxine, Anal. Chem. 75 (2003) 2256–2261.
[5] K. Matsuura, H. Kitakouji, R. Oda, Y. Morimoto, H. Asano, H. Ishida, M. Kiso, K. Kitajima, K. Kobayashi, Selective expansion of the GM3 glycolipid monolayer induced by saccharide-saccharide interaction with Gg3 trisaccharide-bearing glycoconjugate polystyrene at the air-water interface, Langmuir 18 (2002) 6940–6945.
[6] Y. Miura, H. Sato, T. Ikeda, H. Sugimura, O. Takai, K. Kobayashi, Micropatterned saccharide displays self-assembly of glycoconjugate polymers on hydrophobic templates on sillicon, Biomacromolecules 5 (2004) 1708–1713.
[7] Y. Shinohara, Y. Hasegawa, H. Kaku, N. Shibuya, Elucidation of the mechanism enhancing the avidity of lectin with oligosaccharides on the solid phase surface, Glycobiology 7 (1997) 1201–1208.
[8] T. Matsubara, K. Iijima, M. Nakamura, T. Taki, Y. Okahata, T. Sato, Specific binding of GM1-binding peptides to high-density GM1 in lipid membranes, Langmuir 23 (2007) 708–714.
[9] A. Kuno, N. Uchiyama, S. Koseki-Kuno, Y. Ebe, S. Takashima, M. Yamada, J. Hirabayashi, Evanescent-field fluorescence-assisted lectin microarray: a new strategy for glycan profiling, Nat. Methods 2 (2005) 851–856.
[10] O.A. Sadik, F. Yan, Electrochemical biosensors for monitoring the recognition of glycoprotein–lectin interactions, Anal. Chim. Acta. 588 (2007) 292–296.
[11] J.K. Lee, Y.S. Chi, I.S. Choi, Reactivity of acetylenyl-terminated self-assembled monolayers on gold: triazole formation, Langmuir 20 (2004) 3844–3847.
[12] M.C. Bryan, F. Fazio, H.-K. Lee, C.-Y. Huang, A. Chang, M.D. Best, D.A. Calarese, O. Blixt, J.C. Paulson, D. Burton, I.A. Wilson, C.-H. Wong, Covalent display of oligosaccharide arrays in microtiter plates, J. Am. Chem. Soc. 126 (2004) 8640–8641.
[13] K. Sasaki, Y. Nishida, T. Tsurumi, H. Uzawa, H. Kondo, K. Kobayashi, Facile assembly of cell surface oligosaccharide mimics by copolymerization of saccharide modules, Angew. Chem., Int. Ed. 41 (2002) 4463–4467.
[14] S.A. Yamanaka, D.H. Charych, A.L. Douglas, D.Y. Sasaki, Solid phase immobilization of optically responsive liposomes in sol–gel materials for chemical and biological sensing, Langmuir 13 (1997) 5049–5053.
[15] U.H. zawa, S. Kamiya, N. Monoura, H. Dohi, Y. Nishida, K. Taguchi, S.-I. Yokoyama, H. Mori, T. Shimizu, K. Kobayashi, A quartz crystal microbalance method for rapid detection and differentiation of shiga toxins by applying a monoalkyl globobioside as the toxin ligand, Biomacromolecules 3 (2002) 411–414.
[16] Y. Miura, K. Yasuda, K. Yamamoto, M. Koike, Y. Nishida, K. Kobayashi, Inhibition of Alzheimer amyloid aggregation with sulfated glycopolymers, Biomacromolecules 8 (2007) 2129–2134.
[17] A. Kakio, S. Nishimoto, K. Yanagisawa, Y. Kozutsumi, K. Matsuzaki, Interactions of amyloid beta-protein with various gangliosides in raft-like membranes: importance of GM1 ganglioside-bound form as an endogenous seed for Alzheimer amyloid, Biochemistry 41 (2002) 7385–7890.
[18] K. Kerman, Y. Morita, Y. Takamura, E. Tamiya, Escherichia coli single-strand binding protein-DNA interactions on carbon nanotube-modified electrodes from a label-free electrochemical hybridization sensor, Anal. Bioanal. Chem. 381 (2005) 1114–1121.
[19] K. Kerman, N. Nagatani, M. Chikae, T. Yuhi, Y. Takamura, E. Tamiya, Label-free electrochemical immunoassay for the detection of human chorionic gonadotropin hormone, Anal. Chem. 78 (2006) 5612–5616.
[20] M. Takata, K. Kerman, N. Nagatani, H. Konaka, M. Namiki, E. Tamiya, Label-free bioelectronic immunoassay for the detection of human telomerase reverse transcriptase in urine, J. Electroanal. Chem. 596 (2006) 109–116.
[21] M. Vestergaard, K. Kerman, M. Saito, N. Nagatani, Y. Takamura, E. Tamiya, A rapid label-free electrochemical detection and kinetic study of Alzheimer's amyloid beta aggregation, J. Am. Chem. Soc. 127 (2005) 11892–11893.
[22] F. Fazio, M.C. Bryan, O. Blixt, C. James, J.C. Paulson, C.H. Wong, Synthesis of sugar arrays in microtiter plate, J. Am. Chem. Soc. 124 (2002) 14397–14402.
[23] M. Chikae, K. Idegami, K. Kerman, N. Nagatani, M. Ishikawa, Y. Takamura, E. Tamiya, Direct fabrication of catalytic metal nanoparticles onto the surface of a screen-printed carbon electrode, Electrochem. Commun. 8 (2006) 1375–1380.
[24] K. Arihara, T. Ariga, N. Takashima, K. Arihara, T. Okajima, F. Kitamura, K. Tokuda, T. Ohsaka, Multiple voltammetric waves for reductive desorption of cysteine and 4-mercaptobenzoic acid monolayers self-assembled on gold substrates, Phys. Chem. Chem. Phys. 5 (2003) 3758–3761.
[25] M.S. El-Deab, K. Arihara, T. Ohsaka, Fabrication of Au(111)-like polycrystalline gold electrodes and their applications to oxygen reduction, J. Electrochem. Soc. 151 (2004) E213–E218.
[26] T.M. Herne, M.J. Tarlov, Characterization of DNA probes immobilized on gold surfaces, J. Am. Chem. Soc. 119 (1997) 8916–8920.
[27] A.B. Steel, T.M. Herne, M.J. Tarlov, Electrochemical quantitation of DNA immobilized on gold, Anal. Chem. 70 (1998) 4670–4677.
[28] A.B. Steel, T.M. Herne, M.J. Tarlov, Electrostatic interactions of redox cations with surface-immobilized and solution DNA, Bioconjug. Chem. 10 (1999) 419–423.
[29] J. Zhang, Q.J. Chi, J. Ulstrup, Assembly dynamics and detailed structure of 1-propanethiol monolayers on Au(111) surfaces observed real time by in situ STM, Langmuir 22 (2006) 6203–6213.
[30] M.P. Lambert, A.K. Barlow, B.A. Chromy, C. Edwards, R. Freed, M. Liosatos, T.E. Morgan, I. Rozovsky, B. Trommer, K.L. Viola, P. Wals, C. Zhang, C.E. Finch, G.A. Krafft, W.L. Klein, Diffusible, nonfibrillar ligands derived from Aβ1-42 are potent central nervous system neurotoxins, Proc. Natl. Acad. Sci. U. S. A. 95 (1998) 6448–6453.
[31] R. Sighavi, A. Kumar, G.P. Lopez, G.N. Stephanolpoulos, D.I. Wang, G.M. Whitesides, D.E. Ingber, Engineering cell shape and function, Science 264 (1994) 696–698.